Photosynthesis Research (2019) 141:151–163
https://doi.org/10.1007/s11120-019-00616-x

ORIGINAL ARTICLE

Energy transfer from chlorophyll *f* to the trapping center in naturally occurring and engineered Photosystem I complexes

Vasily Kurashov[1] · Ming-Yang Ho[1,2] · Gaozhong Shen[1] · Karla Piedl[1] · Tatiana N. Laremore[4] · Donald A. Bryant[1,2,5] · John H. Golbeck[1,3,6]

Received: 31 October 2018 / Accepted: 11 January 2019 / Published online: 1 February 2019
© Springer Nature B.V. 2019

Abstract

Certain cyanobacteria can thrive in environments enriched in far-red light (700–800 nm) due to an acclimation process known as far-red light photoacclimation (FaRLiP). During FaRLiP, about 8% of the Chl *a* molecules in the photosystems are replaced by Chl *f* and a very small amount of Chl *d*. We investigated the spectroscopic properties of Photosystem I (PSI) complexes isolated from wild-type (WT) *Synechococcus* sp. PCC 7335 and a *chlF* mutant strain (lacking Chl *f* synthase) grown in white and far-red light (WL–PSI and FRL–PSI, respectively). WT–FRL–PSI complexes contain Chl *f* and Chl *a* but not Chl *d*. The light-minus dark difference spectrum of the trapping center at high spectral resolution indicates that the special pair in WT–FRL–PSI consists of Chl *a* molecules with maximum bleaching at 703–704 nm. The action spectrum for photobleaching of the special pair showed that Chl *f* molecules absorbing at wavelengths up to 800 nm efficiently transfer energy to the trapping center in FRL–PSI complexes to produce a charge-separated state. This is ~50 nm further into the near IR than WL–PSI; Chl *f* has a quantum yield equivalent to that of Chl *a* in the antenna, i.e., ~1.0. PSI complexes from *Synechococcus* 7002 carrying 3.8 Chl *f* molecules could promote photobleaching of the special pair by energy transfer at wavelengths longer than WT PSI complexes. Results from these latter studies are directly relevant to the issue of whether introduction of Chl *f* synthase into plants could expand the wavelength range available for oxygenic photosynthesis in crop plants.

Keywords Cyanobacteria · Photosynthesis · Chlorophyll *f* synthase · Action spectrum · Quantum yield · Far-red light photoacclimation · FaRLiP · Photosystem I · Chlorophyll · Cyanobacteria · *Synechococcus* sp. PCC 7002 · *Synechococcus* sp. PCC 7335

Introduction

Terrestrial cyanobacteria often occupy light niches that are highly enriched in far-red light (FRL, specifically wavelengths between 700 and 800 nm). These may include soils, rocks, caves, microbial mats, and environments shaded by plants (Gan et al. 2014; Ho et al. 2017c). Either by physical

Electronic supplementary material The online version of this article (https://doi.org/10.1007/s11120-019-00616-x) contains supplementary material, which is available to authorized users.

✉ John H. Golbeck
jhg5@psu.edu

[1] Department of Biochemistry and Molecular Biology, The Pennsylvania State University, University Park, PA 16802, USA

[2] Intercollege Graduate Degree Program in Plant Biology, The Pennsylvania State University, University Park, PA 16802, USA

[3] Department of Chemistry, The Pennsylvania State University, University Park, PA 16802, USA

[4] Proteomics and Mass Spectrometry Core Facility, The Huck Institutes for the Life Sciences, The Pennsylvania State University, University Park, PA 16802, USA

[5] Department of Chemistry and Biochemistry, Montana State University, Bozeman, MT 59717, USA

[6] 328 South Frear Laboratory, Department of Biochemistry and Molecular Biology, The Pennsylvania State University, University Park, PA 16802, USA

processes, such as light scattering, or by strong filtration of light by the absorbance of chlorophyll (Chl) *a*, these niches can be largely devoid of visible light. Nevertheless, some cyanobacteria can thrive in such environments due to an acclimation process known as far-red light photoacclimation (FaRLiP) (Gan et al. 2014; Ho et al. 2017c). During FaRLiP, a conserved cluster of 20 genes is very highly expressed (Gan et al. 2014; Zhao et al. 2015). This cluster encodes FRL-specific core subunits of photosystem II (PSII), photosystem I (PSI), and phycobilisomes (PBS) (Gan et al. 2014; Ho et al. 2017a, b, c; Herrera-Salgado et al. 2018). In FRL, six membrane-intrinsic Chl-binding subunits of PSI are specifically replaced by paralogous subunits from the FaRLiP gene cluster (PsaA2, PsaB2, PsaF2, PsaI2, PsaJ2, and PsaL2) (Gan et al. 2014). Similarly, five membrane-intrinsic Chl-binding subunits of PSII are replaced by paralogs from the FaRLiP gene cluster (PsbA3, PsbB2, PsbC2, PsbD3, and PsbH2). Two new Chls are additionally produced, Chl *d* and Chl *f* (Airs et al. 2014; Gan et al. 2014; Gan and Bryant 2015; Ho et al. 2016). These combined changes in pigmentation, gene expression, and complex structure lead to extensive remodeling of the photosynthetic apparatus in FaRLiP organisms, and these changes allow FaRLiP organisms to perform oxygenic photosynthesis using FRL.

PSI is a supramolecular membrane protein complex that typically comprises 11 or 12 polypeptides (PsaA, PsaB, PsaC, PsaD, PsaE, PsaF, PsaI, PsaJ, PsaK, PsaL, PsaM, PsaX) (Golbeck and Bryant 1991). It is a light-driven oxidoreductase that binds 96 Chl *a* molecules, 22 β-carotene molecules, 2 phylloquinone (or menaquinone-4) molecules, and three [4Fe-4S] clusters, denoted F_X, F_A, and F_B (Jordan et al. 2001; Grotjohann and Fromme 2005). PSI uses light to oxidize a weak reductant (reduced plastocyanin or cytochrome c_6, E_m ca. +350 mV) in order to produce a strong reductant (reduced ferredoxin or flavodoxin, E_m ca −420 mV) [Fig. S1; (Golbeck and Bryant 1991)]. The Chls are exclusively Chl *a* in most cyanobacterial PSI complexes; 90 Chl *a* molecules form the core antenna, while six Chl *a* molecules form a pseudo-symmetric, branched electron transport chain (Fig. S1). The nature of the primary electron donor remains a matter of debate. Traditionally, charge separation in PSI has been thought to originate at the special pair known as P_{700}, but one study indicates that it may occur between a monomeric accessory Chl *a* (either Chl ec-A2 or ec-B2), and a monomeric Chl *a* acceptor known as A_0 (ec-A3 or ec-B3). In the latter case, the resulting hole on the Chl *a* cation migrates to the Chl *a*/Chl *a′* special pair (Müller et al. 2010), which is spectroscopically known as P_{700} because of the wavelength at which maximal bleaching occurs (Kok 1956). PSI is remarkably efficient in converting light energy into stored chemical potential energy. This efficiency is achieved by utilizing a multi-component, electron transport chain that rapidly transfers an electron from P_{700} on one side of the thylakoid membrane to the F_A/F_B clusters on the other, a center-to-center distance of ~43 Å (Jordan et al. 2001). The overall quantum efficiency for this process is essentially 100%, and ~35 to 40% of the energy of a red photon is stored as quasi-stable, chemical potential energy (Golbeck 2006; Mielke et al. 2013).

About 20 years ago, an unusual cyanobacterium, *Acaryochloris marina*, was discovered that produces predominantly Chl *d* (Chl *a* with the 3-vinyl side chain replaced by a formyl moiety), which causes the Q_y absorption maximum to red-shift to about 695 nm in methanol (Miyashita et al. 1996; Chen 2014). Studies with PSI from *A. marina* established that the primary electron donor exhibits maximal photobleaching at 740 nm, which indicated that the special pair for these complexes includes Chl *d*. The discovery of Chl *d′* and further spectroscopic studies showed that the special pair in the PSI of *A. marina* is a Chl *d*/Chl *d′* heterodimer (Sivakumar et al. 2003; Tomo et al. 2008; Allakhverdiev et al. 2016). The PSI complexes of *A. marina* also contain a very small amount of Chl *a*; transient absorbance measurements suggest that Chl *a* is likely the primary electron acceptor (Kumazaki et al. 2002; Itoh et al. 2007). PSII complexes of *A. marina* contain ~29.6 Chl *d* and 1.9 Chl *a* molecules per 2.0 pheophytin (Pheo) *a* molecules (Allakhverdiev et al. 2010). Although Pheo *a* is recognized as the primary electron acceptor (Razeghifard et al. 2005; Schlodder et al. 2007; Tomo et al. 2007), after more than 20 years of study and debate, the exact Chl composition of the primary donor of these PSII complexes remains controversial and unresolved (Allakhverdiev et al. 2016).

During FaRLiP, about 8% of the Chl *a* molecules in the photosystems are replaced by Chl *f*, and a small amount of Chl *d* (~1%) is produced (Gan et al. 2014; Ho et al. 2017c; Ho 2018). Recent studies have shown that Chl *f* is associated with both PSI and PSII, but Chl *d* is exclusively associated with PSII (Ho 2018; Nurnberg et al. 2018). In the studies reported here, we have investigated the spectroscopic properties of FRL–PSI complexes in the wild-type (WT) strain of *Synechococcus* sp. PCC 7335. Firstly, we have verified that WT–FRL–PSI complexes do not contain Chl *d*. Secondly, we measured the light-induced absorbance difference spectrum of the trapping center at high spectral resolution (~1 nm) to determine whether Chl *a*/Chl *a′* or Chl *f*/Chl *f′* (or both) might be components. Thirdly, we measured the action spectrum for photobleaching of the special pair to determine the wavelength range over which Chl *f* can absorb light and promote charge separation in isolated WT–FRL–PSI complexes. Finally, we studied PSI complexes from *Synechococcus* sp. PCC 7002 carrying 3.8 Chl *f* molecules to determine whether bound Chl *f* molecules could promote photobleaching of the special pair by energy transfer. Results from these latter studies are directly relevant to

the issue of whether introduction of Chl *f* synthase into plants could expand the wavelength range of light available for oxygenic photosynthesis in crop plants.

Materials and methods

Strains and growth conditions

Synechococcus sp. PCC 7002 (hereafter *Synechococcus* 7002) and engineered strains for heterologous expression of the *chlF* gene of *Fischerella thermalis* PCC 7521 [hereafter *F. thermalis* 7521; (Shen et al. 2019)] were grown in liquid A^+ medium under standard conditions as previously described: 250 µmol photons m^{-2} s^{-1} cool-white fluorescent light, 38 °C, and sparging with 1% (v/v) CO_2 in air (Ludwig and Bryant 2011). *Synechococcus* 7002 strains in which the *psbD1* and *psbD2* genes had been deleted (Shen et al. 2019) were grown under lower irradiance (~ 10 µmol photons m^{-2} s^{-1}), and the medium was supplemented with 20 mM glycerol (Lambert and Stevens 1986). Antibiotics were added as required at the following concentrations: gentamycin (50 µg ml^{-1}); spectinomycin (100 µg ml^{-1}); and kanamycin (100 µg ml^{-1}).

Synechococcus sp. PCC 7335 (hereafter *Synechococcus* 7335) was obtained from the Pasteur Culture Collection (http://www.pasteur.fr/pcc_cyanobacteria; (Rippka et al. 1979). Cells were grown at room temperature (~ 25 °C) in ASN-III medium supplemented with vitamin B_{12} (4 µg l^{-1}) and 10 mM Tris–HCl, pH 8.0). The *chlF* mutant was generated by replacing the *chlF* gene with an *aphAII* gene for kanamycin resistance (Ho et al. 2016) and was grown by supplementing the medium with kanamycin (50 µg ml^{-1}). This mutant only accumulates Chl *a* even when grown in FRL (Suppl. Fig. S2). *Synechococcus* 7335 does not tolerate high white light intensities (WL) and was routinely grown at ~ 25 to 100 µmol photons m^{-2} s^{-1}. Lower irradiance values were achieved either by varying the number of cool-white fluorescent tubes or by using neutral density filters. An LED panel (L720-06AU; Marubeni, Santa Clara, CA, USA) with emission centered at 720 nm and/or a halogen light filtered by a combination of green and red plastic filters were used to provide far-red light at ~ 180 µmol photons m^{-2} s^{-1} (Gan et al. 2014; Ho et al. 2016, 2017a, b). Cell growth was monitored as optical density at 750 nm by using a GENESYS 50 spectrophotometer (ThermoSpectronic, Rochester, NY).

Purification of trimeric Photosystem I complexes

PSI was purified on sucrose gradients as described previously with minor modifications (Gan et al. 2014). *Synechococcus* 7335 cells cultured under different light conditions were harvested and resuspended in MES buffer (50 mM MES, pH 6.5, 10 mM $CaCl_2$, and 10 mM $MgCl_2$). Resuspended cells were broken by three passages through a French pressure cell at 138 MPa at 4 °C as previously described. After centrifugation at 3830×*g* at 4 °C for 10 min to remove unbroken cells and cell debris, thylakoid membranes were pelleted by ultracentrifugation at 126,100×*g* at 4 °C for 30 min. The thylakoid membranes were resuspended in MES buffer. The Chl concentration was adjusted to 0.4 mg Chl ml^{-1}, and the thylakoid membranes were solubilized in 1% (w/v) *n*-dodecyl-β-D-maltoside (DM) at 4 °C for 1 h. After centrifugation at 15,294×*g* at 4 °C for 10 min, the supernatant was loaded onto a 10–20% (w/v) sucrose gradient containing 0.02% (w/v) DM. The gradient was centrifuged in a swinging bucket rotor at 133,900×*g* at 4 °C for 18 h. The lowest green band in the sucrose gradient contained PSI trimer complexes that were collected for further analysis (see below).

PSI complexes were purified from the wild-type (WT) strain of *Synechococcus* 7002 and from *ΔpsbD1 ΔpsbD2* mutant cells harboring plasmid pAQ1Ex::$chlF^{7521}$ (Gm^R) by following similar procedures (Shen and Bryant 1995; Shen et al. 2002, 2016, 2019). Trimeric PSI complexes were collected from the lowest regions of the sucrose gradients, dialyzed against MES buffer and concentrated using the Millipore Centriprep 100K Centrifugal Filter Devices (EMD Millipore, Darmstadt, Germany). The concentrated PSI complexes were sometimes purified further by ultracentrifugation on similar sucrose gradients lacking added DM. Purified PSI complexes were resuspended in MES buffer containing 0.05% (w/v) DM and 5% (w/v) glycerol.

Pigment extraction and analysis

Cyanobacterial cells were harvested by centrifugation and washed once in 50 mM HEPES pH 7.2 prior to pigment extraction and analysis. Pigments were extracted from cells and purified PSI complexes by sonication in the dark with acetone/methanol (7:2, v/v) containing iodoacetamide (10 µl of a 36 mg ml^{-1}stock solution). After centrifugation to remove cell debris and/or precipitated proteins, pigment extracts were filtered using Whatman™ 0.2 µm polytetrafluoroethylene syringe filters (GE Healthcare Life Sciences, Boston, MA) and analyzed by reversed-phase, high-performance liquid chromatography (HPLC) on an Agilent 1100 HPLC system with a Model G1315B diode-array detector (Agilent Technologies, Santa Clara, CA) equipped with an analytical Discovery C18 column (4.6 mm × 25 cm) (Supelco, Sigma-Aldrich, St. Louis, MO), following the solvent programs described previously (Gan et al. 2014; Gan and Bryant 2015). An alternative HPLC analysis method was sometimes used as described previously (Ortega-Ramos

et al. 2018). Pigment extracts were filtered and buffered by addition of 0.1 volume of 1.0 M ammonium acetate before injection onto the HPLC column. Solvents A and B were 64:16:20 (v/v/v) methanol/acetone/H_2O and 80:20 (v/v) methanol/acetone, respectively. To detect species of Chl *a, d*, and *f* as well as carotenoids, the absorbance spectra of all eluted compounds were collected between 350 and 900 nm at 0.5-s intervals. The HPLC data were processed using Agilent ChemStation software (revision B.02.01-SR1 6100 series).

In-solution trypsin digestion and LC–MS–MS protein identification

Fractions containing PSI complexes isolated from sucrose gradient centrifugation from cells grown in WL or FRL of the WT and *chlF* mutant strains of *Synechococcus* 7335 were analyzed at the Proteomics and Mass Spectrometry core facility of the Huck Institutes for the Life Sciences at The Pennsylvania State University, University Park, as previously described (Ho et al. 2017a, b, c; Ho 2018). In-solution samples digested with trypsin were analyzed by LC–MS–MS on a Thermo LTQ Orbitrap Velos ETD mass spectrometer equipped with a Dionex UltiMate 3000 Nanoflow 2D LCY system.

Absorption and fluorescence spectroscopy and pigment content determination

Absorption spectra of isolated PSI complexes at room temperature were measured using a Varian Cary 50 UV–Vis spectrophotometer. The 0.2 × 1.0 cm cuvette was oriented to include a 0.2 cm optical path. Absorption spectra and fluorescence emission spectra at 77 K were measured as previously described (Shen et al. 2008, 2019). Chls were extracted from cells or purified PSI complexes with 100% methanol. Chl *a* and Chl *f* concentrations were determined from absorption spectra of extracts from the Q_y absorption band of Chl *a* at 665 nm and of Chl *f* at 707 nm, using the molar extinction coefficients in methanol for Chl *a* (70.54 mM^{-1} cm^{-1}; (Lichtenthaler 1987)), Chl *d* (63.68 mM^{-1} cm^{-1}; (Li et al. 2012)) and Chl *f* (71.11 mM^{-1} cm^{-1}; (Li et al. 2012)).

Measurement of light-induced difference spectra

Light-induced difference spectra were measured using a setup based on modified Varian Cary 50 UV–Vis spectrophotometer. A Newport 66902 arc lamp outfitted with a 400 W xenon lamp provided the actinic light, which was first passed through a circulating water filter to reduce sample heating. An optical fiber with an outboard shutter directed the light to the cuvette holder at a 90° angle to the probe beam. The amount of light absorbed at a given wavelength was measured with the shutter closed for 2 min (the dark signal) and with the shutter open (the light signal); the difference between the light and dark signals was plotted against the corresponding wavelength. A recovery period long enough for the sample to return to the ground state followed each measurement. A 0.4 × 1.0 cm cuvette held the sample, which was oriented so that the measuring beam passed through the 1 cm optical path and the actinic beam passed through the 0.4 cm path. The light intensity was adjusted by altering the power to the lamp and fine-tuned with neutral density filters to achieve the minimum saturating power, *i.e.*, the power at which any further increase in the light intensity showed no increase in the absorbance change.

Measurement of light intensity to achieve 50% saturation of the trapping center

The amount of light required to achieve 50% saturation of the trapping center was measured at wavelengths from 650 to 795 nm using the laboratory build setup described above and an assortment of narrow-band interference filters with full width at half maxima of 7 to 10 nm. All measurements were made at 700 nm. Prior to measurement, saturating white light was used to determine the maximum absorbance change possible for a given sample. Immediately thereafter, an interference filter was positioned in front of the actinic light source, and the light intensity was attenuated to reach the 50% of the maximum absorbance change. The light intensity was measured using a calibrated Newport 843-R power meter equipped with a Newport 918D-SL-OD3R detector. The measured light intensity was corrected for the sample absorbance (see below) and plotted against the corresponding filter transmittance maximum wavelength. The inverse of these data represents the action spectrum of the sample. The ratio of the normalized action spectrum and absorbance spectrum then represents the relative quantum efficiency.

Correction for actinic light intensity

When the actinic beam (I_0) passes through the sample, its intensity decreases due to absorption by the pigments (Fig. 1). Because measurement of the absorbance is carried out in a small slice in the middle of the optical path of the actinic light, it is necessary to calculate the amount of light absorbed by the sample in this region of the cuvette. This is done using formula (1), where $\boldsymbol{\varepsilon}$ is the extinction coefficient, $\boldsymbol{c}$ is the concentration of the sample, and L_1 is the optical path from the surface of the sample to the probing beam area.

$$I = I_0 \cdot 10^{-\varepsilon \cdot c \cdot L_1} \quad (1)$$

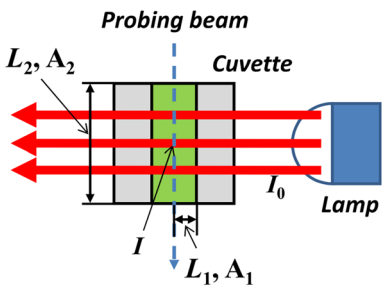

Fig. 1 Depiction of the measuring and actinic beams relative to the dimensions of the cuvette. The probe beam is relatively narrow and passes through the middle of the cuvette, and hence the intensity of the actinic beam is diminished by absorption from pigments

$\varepsilon{\cdot}c$ is calculated using formula (2), where A_2 is the absorbance of the sample measured through the optical path L_2.

$$\varepsilon \cdot c = \frac{A_2}{L_2} \tag{2}$$

If $\varepsilon{\cdot}c$ from formula (2) would be used in formula (1), I can be calculated using formula (3).

$$I = I_0 \cdot 10^{-\frac{A_2}{L_2} \cdot L_1} \tag{3}$$

An absorbance spectrum was recorded prior to the measurement in a cuvette with a 0.2 cm optical path (L_2) that was equal to L_1 and A_2 was taken from that spectrum. Formula (4) is the final formula used for the light correction, where A_{xxx} was the absorbance at the wavelength *xxx* nanometers equal to the transmittance maximum of the filter in use.

$$I = I_0 \cdot 10^{-A_{xxx}} \tag{4}$$

Results

Isolation and characterization of Photosystem I complexes from *Synechococcus* 7335 strains

Figure 2a shows sucrose gradients that were used to fractionate solubilized thylakoid membranes prepared from *Synechococcus* 7335 WT cells grown in WL or FRL. The complexes showing the farthest migration on the gradients were in each case similar in migration to well-characterized trimeric PSI complexes from numerous other cyanobacteria, including *Synechococcus* 7002 and *Synechocystis* sp. PCC 6803 (Shen and Bryant 1995; Schluchter et al. 1996; Shen et al. 2002, 2016, 2019). Electron microscopy of negatively stained preparations showed that these fractions contained trimeric PSI complexes (data not shown). Figure 2b, c, respectively, shows the absorption and low-temperature

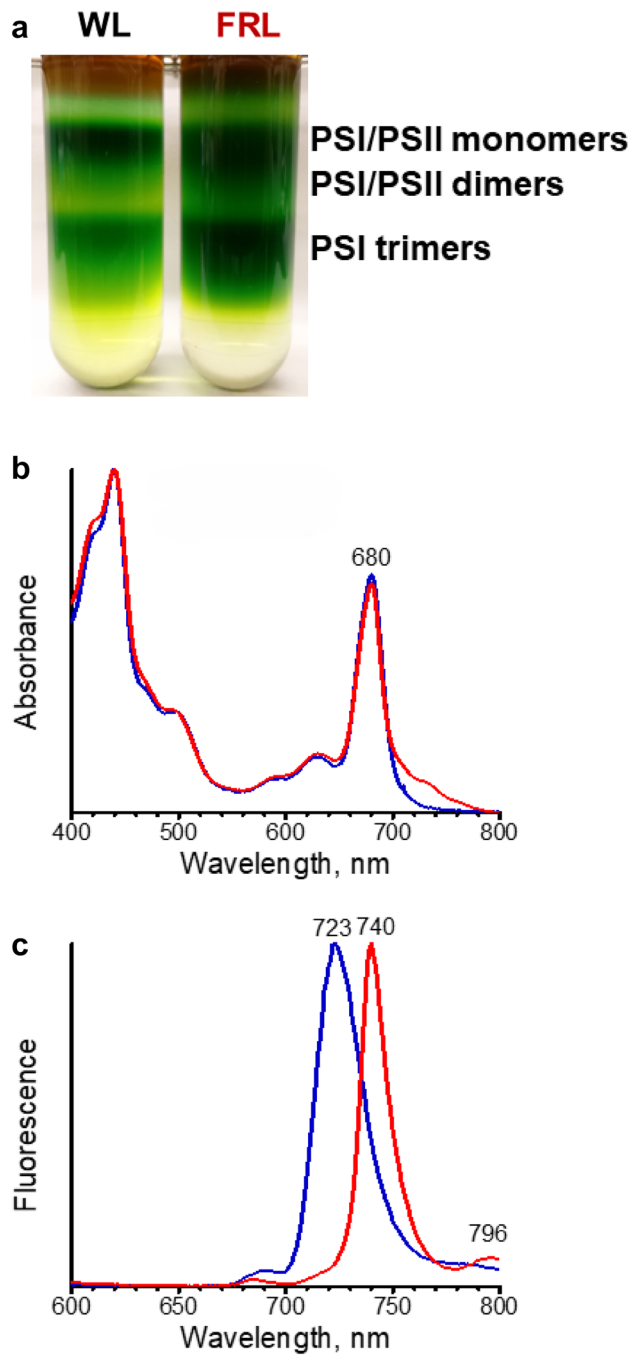

Fig. 2 Isolation and spectroscopic properties of trimeric PSI complexes from WT *Synechococcus* 7335. **a** Sucrose density gradients showing the fractionation of solubilized thylakoid membranes from cells grown in white light (WL) and far-red light (FRL). The monomeric, dimeric, and trimeric fractions containing the indicated PSI and PSII complexes are indicated on the figure. The bands containing PSI and PSII on the top of the gradients have been analyzed by spectroscopy and native PAGE, and the monomer and dimer bands obtained by native PAGE have been subjected to LC–MS/MS analyses. The results indicated clearly that the upper two fractions of the sucrose density gradients contain both PSI and PSII. **b** Absorbance spectra for isolated trimeric PSI complexes from cells grown in WL (blue line) or FRL (red line). **c** Fluorescence emission spectra at 77 K of isolated trimeric PSI complexes from cells grown in WL (blue line) or FRL (red line). The excitation wavelength was 440 nm

fluorescence emission spectra of these two fractions. The WT–WL–PSI and WT–FRL–PSI complexes both had Q_y absorbance maxima at 680 nm but the fluorescence emission maximum for the WT–WL–PSI complexes was 723 nm while the WT–FRL–PSI complexes exhibited emission maxima at 740 nm and 796 nm. The Chl content of these complexes was assessed by reversed-phase HPLC. As shown in Table S1, the WT–WL–PSI complexes contained no Chl *d* or Chl *f* and only contained Chl *a*. The WT–FRL–PSI complexes contained 87.6 Chl *a* and 8.4 Chl *f* molecules, but these complexes contained $\leq 0.3 \pm 0.1$ Chl *d* molecule per PSI monomer. Tryptic peptide mass fingerprinting was used to identify the PSI-related proteins associated each of these fractions. As shown in Table S2, the WL–PSI complexes contained PSI subunits PsaA1, PsaB1, PsaD, PsaE, PsaF1, PsaI1, PsaJ1, PsaK, and PsaL1 but did not contain detectable amounts of the PSI proteins encoded by the FaRLiP gene cluster. In contrast, the FRL–PSI complexes contained PsaA2, PsaB2, PsaD, PsaE, PsaF2, PsaK, and PsaL2. A very small amount of PsaF1 was detected in these complexes as well, but no other paralogous subunits encoded by genes outside the FaRLiP gene cluster were detected in the FRL–PSI complexes from the WT strain.

Figure 3 shows similar results for the *chlF* null mutant of *Synechococcus* 7335 that is unable to synthesize Chl *f* (Suppl. Fig. S2) (Ho et al. 2016). The WL–PSI complexes from this mutant have absorption and fluorescence emission spectra that are virtually identical to those of the WT strain (compare Fig. 2b, 2c and 3b, 3c). However, the FRL–PSI complexes from the *chlF* mutant are also very similar, if not identical, to those of the WT or *chlF* mutant strains grown in WL. Notably, the low-temperature fluorescence emission maximum for the FRL–PSI complexes had an emission maximum at 722 nm, not 740 nm as observed for the FRL–PSI complexes from the WT strain (Figs. 2c and 3c). Tryptic peptide mass fingerprinting confirmed that the FRL–PSI complexes did not contain proteins encoded by the FaRLiP gene cluster (Table S2). Instead, the FRL–PSI complexes of the *chlF* mutant contained the same subunits as found in PSI complexes from the WT strain and *chlF* mutant strains grown in WL. Thus, Chl *f* is apparently required for the assembly and/or stable accumulation of FRL–PSI complexes, and only PSI complexes similar to those produced in WL were found in the *chlF* mutant cells grown in FRL. It should also be noted that the PSI complexes produced in FRL were mostly monomeric and yields of trimeric PSI were quite low from the *chlF* mutant strain (Fig. 3a).

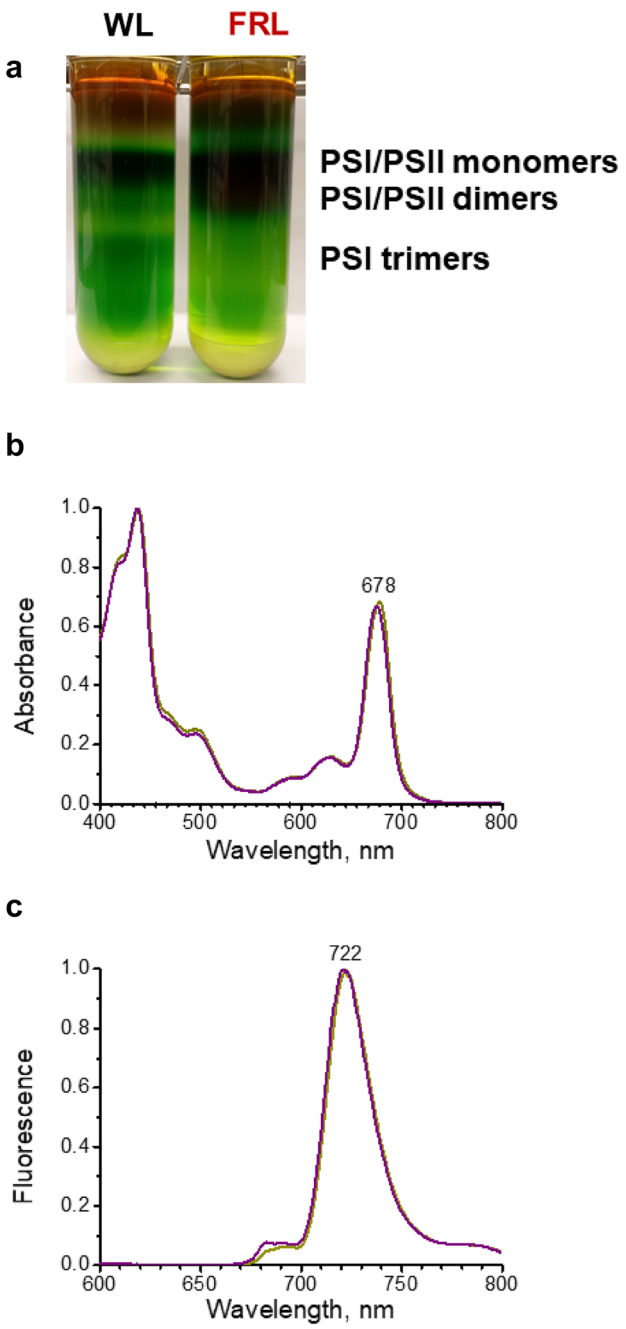

Fig. 3 Isolation and spectroscopic properties of trimeric PSI complexes from the *chlF* mutant of *Synechococcus* 7335 that is unable to synthesize Chl *f*. **a** Sucrose density gradients showing the fractionation of solubilized thylakoid membranes from cells grown in white light (WL) and far-red light (FRL). The monomeric, dimeric, and trimeric fractions containing the indicated PSI and PSII complexes are indicated according to results of spectroscopic analyses and by comparison with the gradients shown in Fig. 2a. Note the very low yield of PSI trimers in cells grown in FRL. **b** Absorbance spectra for isolated trimeric PSI complexes from the *chlF* mutant cells grown in WL (brown line) or FRL (purple line). Note the absence of absorption in the FRL sample at wavelengths from 700 to 800 nm. **c** Fluorescence emission spectra at 77 K of isolated trimeric PSI complexes from cells grown in WL (brown line) or FRL (purple line). Note the absence of emission at 740 nm for the PSI complexes from FRL. The excitation wavelength was 440 nm

Properties of Photosystem I complexes from *Synechococcus* 7002 strains

Figure 4 shows absorption and low-temperature fluorescence emission spectra for PSI complexes isolated from the WT strain of *Synechococcus* 7002 as well as two strains expressing the *chlF*^{7521} gene from *F. thermalis* 7521. In the first strain, the *chlF*^{7521} gene is expressed from the strong *cpcBA* promoter from *Synechocystis* sp. PCC 6803 in plasmid pAQ1Ex in the WT genetic background (Shen et al. 2019). The 7002 pAQ1Ex::*chlF*^{7521} strain accumulates about 1% Chl *f*, and correspondingly, trimeric PSI complexes contain about 0.9 molecule of Chl *f* on average per PSI monomer (Table S1). In the second strain, the *chlF*^{7521} gene was similarly expressed in a strain devoid of PsbD1, PsbD2, and PSII activity (Shen et al. 2019). The percentage of Chl *f* that accumulates in this strain is ~2% in cells grown in FRL (Table S1). PSI complexes isolated from these cells contain about 3.8 Chl *f* molecules per PSI monomer (Table S1).

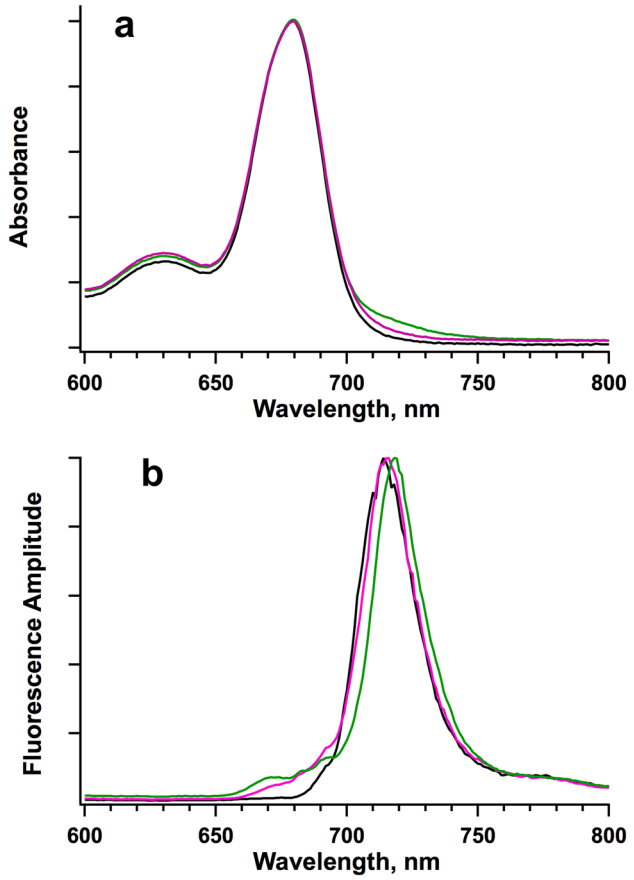

Fig. 4 Absorption spectra (**a**) and fluorescence emission spectra at 77 K (**b**) of isolated PSI complexes from WT *Synechococcus* 7002 and strains heterologously expressing the *chlF*^{7521} gene. Trimeric PSI complexes were purified from cells grown in WL for WT *Synechococcus* 7002 (black line) and for the strain expressing the *chlF*^{7521} gene in a WT background and containing ~1 Chl *f* molecule per monomer (pink line). PSI complexes isolated from the *ΔpsbD1 ΔpsbD2* strain of *Synechococcus* 7002 heterologously producing ChlF^{7521} and containing ~3.8 Chl *f* molecules per PSI monomer (green line) were isolated from cells grown in FRL. For the low-temperature fluorescence emission measurements, the excitation wavelength was 440 nm

In the FRL–PSI complexes from WT *Synechococcus* 7335 cells grown in FRL, the absorption due to the eight Chl *f* molecules in the PSI complexes is readily apparent in the region from 700 to 800 nm (Fig. 2b). There is a long, tailing absorption feature that exhibits hints of finer structure with shoulders at approximately 720, 740, and 760 nm. Additional absorption beyond 700 nm was also clearly evident in the spectrum of PSI complexes from the *Synechococcus* 7002 mutant strain containing the largest amount of Chl *f* (Fig. 4a). However, the absorbance from Chl *f* clearly did not extend as far into the far-red/near-infrared region—only to about 740 nm. The low-temperature fluorescence emission maximum of these PSI complexes red-shifts slightly from 714 nm for WT to 718 nm when 3.8 molecules of Chl *f* were present (Fig. 4b).

Light-induced difference spectrum of the trapping center

To determine if the trapping center consists of a Chl *f*/Chl *f′* special pair, we measured the light-induced difference spectra for WL–PSI and FRL–PSI complexes from WT *Synechococcus* 7335 and compared the results to those for PSI complexes isolated from WT *Synechococcus* 7002, which can only synthesize Chl *a*. Figure 5 shows the light-induced difference spectra for these three PSI complexes for the region 500 to 900 nm. The difference spectra are very similar, and all three complexes exhibit maximal photobleaching near 700 nm. Notably, no significant bleaching is observed from about 720 to 760 nm for the FRL–PSI complexes, the region where photobleaching of Chl *f* would be expected to occur if it were a component of the special pair. Figure 6a shows high-resolution (±1 nm) light-induced difference spectra for FRL–PSI and WL–PSI complexes derived from *Synechococcus* 7335 strains as well as PSI complexes isolated from WT *Synechococcus* 7002. Figure 6b shows light-induced difference spectra for WL–PSI from WT *Synechococcus* 7335 and WL–PSI and FRL–PSI complexes from the *chlF* mutant that cannot synthesize Chl *f* (Ho et al. 2016). The data indicate that there is no significant difference between the photobleaching maximum for PSI complexes from *Synechococcus* 7335 grown in WL (WL–PSI) and for WL–PSI and FRL–PSI complexes from the *chlF* mutant: all PSI complexes have photobleaching maxima at 699 to 700 nm (Fig. 6a, b). However, the light-induced photobleaching maximum for FRL–PSI complexes from *Synechococcus* 7335 WT was reproducibly slightly red-shifted to 703 to 704 nm (Fig. 6a). This shift is too small to derive from a Chl *f*/Chl *f′* special pair, and strongly suggests that the

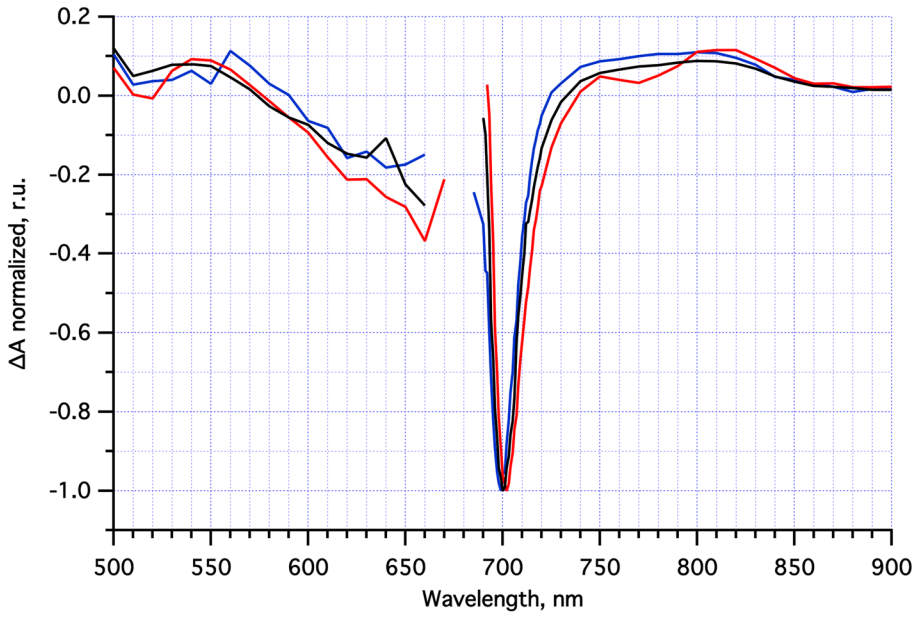

Fig. 5 Light-induced difference spectra of PSI complexes measured at wavelengths from 500 nm to 900 nm in the presence of 10 mM sodium ascorbate and 10 µM DCPIP. PSI complexes isolated from WT *Synechococcus* 7335 grown under WL (blue line) or FRL (red line) and from WT *Synechococcus* 7002 (black line). The gap in the data is near the Chl *a* peak, where the high absorbance of the sample precludes an accurate estimate of the difference spectrum

special pair is a Chl *a*/Chl *a′* heterodimer (Webber and Lubitz 2001), albeit in a different structural environment than P_{700} in WT–WL–PSI complexes. In comparison, WL–PSI from *Synechococcus* 7002 shows a maximum bleaching at 701 nm. Note that for all three samples, the error bars are typically larger on the shorter wavelength edge of the photobleaching peak; the signal-to-noise ratio in this wavelength range is lower because less light reaches the detector due to the much absorbance by Chl *a* at these wavelengths (points around 675 nm were deleted altogether for the spectra shown in Fig. 5). Figure 6c shows that the light-induced difference spectra of PSI complexes isolated from WT *Synechococcus* 7002 overlay exactly with those from strains of *Synechococcus* 7002 containing ~0.9 Chl *f* and 3.8 Chl *f* molecules: all show maximal photobleaching at 700 to 701 nm. These data further support the conclusion that P_{700}^{+} is associated with Chl *a*, likely a Chl *a*/Chl *a′* heterodimer, in all of the PSI complexes studied here. They also show that the photobleaching maximum is a function of the protein expressed, which is different for the three samples shown in Fig. 6a.

Light saturation characteristics of the trapping center

If Chl *f* is capable of transferring energy to the trapping center, then the amount of light necessary to bleach the special pair should be related to the absorbance of the pigment(s) in a particular region of the spectrum. We quantified this by measuring the light intensity, in µW, required to achieve 50% bleaching of the special pair as a function of wavelength. Figure 7a presents these results for wavelengths from 650 nm to 800 nm for PSI complexes isolated from WT and *chlF* mutant strains of *Synechococcus* 7335 strains grown under WL and FRL. The spectra were shifted on the *Y*-axis by a constant to be equivalent at 680 nm and the light intensity is plotted on a log scale. There is no significant difference between the PSI complexes of *Synechococcus* 7335 WT grown under WL and the *chlF* null mutant of *Synechococcus* 7335 grown in WL or FRL. For purposes of comparison, results for PSI complexes isolated from WT *Synechococcus* 7002 are also shown. In these samples, which only contain Chl *a* (Table S1), it was possible to achieve 50% charge separation at wavelengths as long as 735 to 750 nm, although the amount of light required to produce 50% charge separation at 750 nm was ~500 times that required at the peak absorbance wavelength of 680 nm. Large increases in the amount of light necessary for excitation at 760 nm were previously found in WT *Synechocystis sp*. PCC 6803 using femtosecond spectroscopy (Cherepanov et al. 2017a, b). However, in FRL–PSI complexes isolated from WT *Synechococcus* 7335, the response was red-shifted by ~45 nm. In particular, the amount of light required at 750 nm was only 8 to 9 times that required at the peak wavelength of 680 nm, and 50% charge separation could be achieved at wavelengths as long as 795 nm, compared to 750 nm for the other samples. Even at this wavelength, the amount of light required to achieve 50% charge separation was only 120 times that required at the peak wavelength of 680 nm. Consistent with the absorption spectra of cells and FRL–PSI complexes, it is clear that the Chl *f* and Chl *a* molecules in FRL–PSI complexes from WT *Synechococcus* 7335 are able to transfer energy efficiently to the trapping center at much longer wavelengths than the Chl *a* molecules in WL–PSI complexes of WT *Synechococcus* 7335. For these PSI complexes, the longest wavelength at which 50% charge separation was observed was red-shifted by ~45 nm.

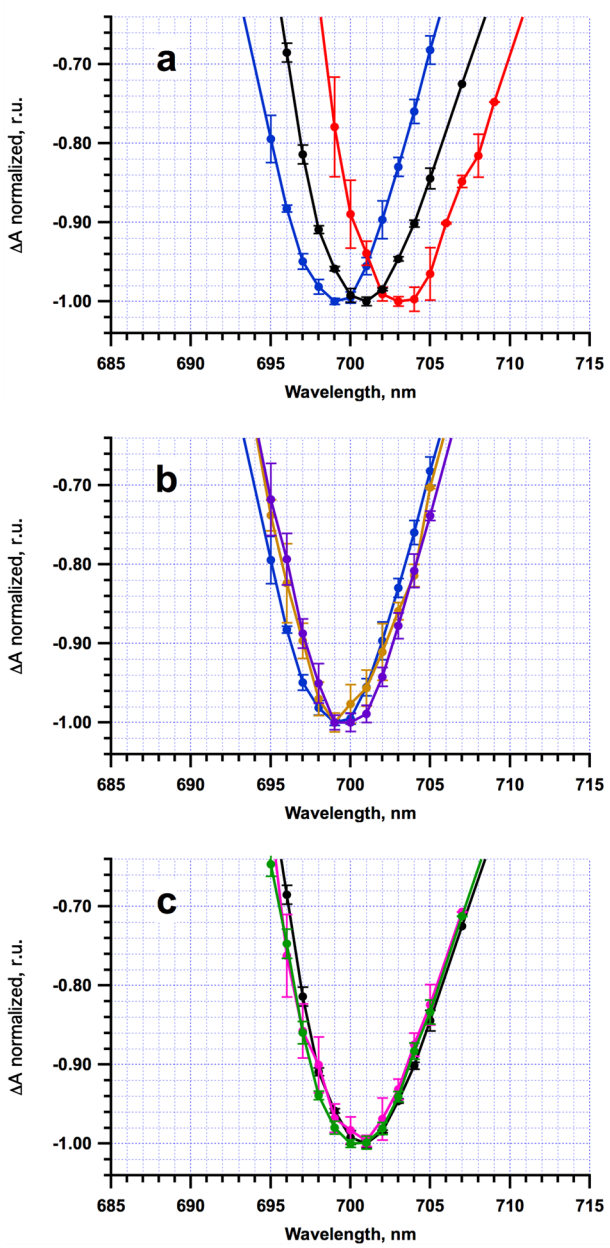

Fig. 6 Light-induced photobleaching spectra of PSI complexes measured at higher resolution (~1 nm) from 693 to 712 nm in the presence of 10 mM sodium ascorbate and 10 µM DCPIP. **a** PSI complexes isolated from *Synechococcus* 7335 grown under WL (blue line) and FRL (red line), and PSI complexes isolated from WT *Synechococcus* 7002 (black line). **b** PSI complexes isolated from *Synechococcus* 7335 grown under WL (blue line) and from the *chlF* deletion mutant of *Synechococcus* 7335 grown under WL (brown line) and FRL (purple line). **c** PSI complexes isolated from WT *Synechococcus* 7002 (black line), from WT *Synechococcus* 7002 heterologously producing ChlF^{7521} and containing ~1 Chl *f* molecule per PSI monomer (pink line), and from the *ΔpsbD1 ΔpsbD2* strain of *Synechococcus* 7002 heterologously producing ChlF^{7521} and containing ~3.8 Chl *f* molecules per PSI monomer (green line). The error bars are largest in the regions where the sample has the most absorption

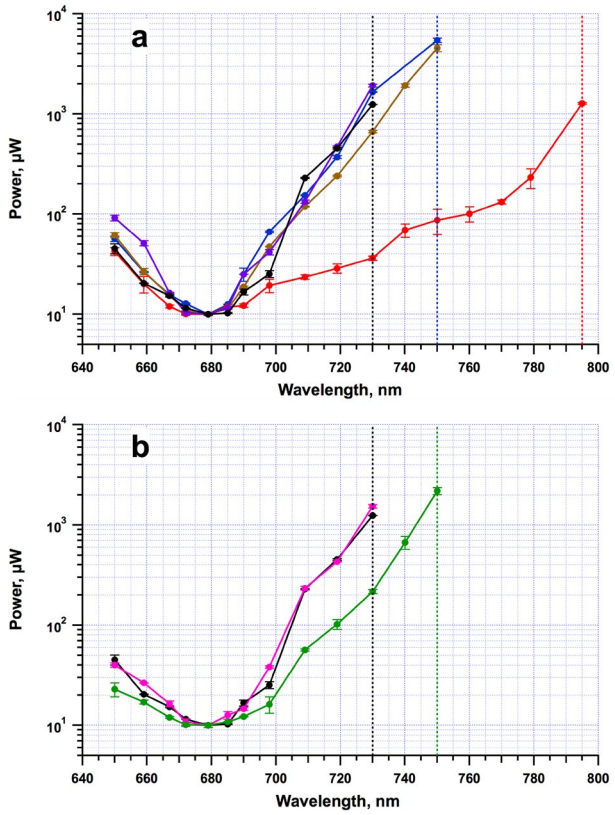

Fig. 7 Amount of light necessary to bleach 50% of the trapping center measured as a function of wavelength. Details are provided in "Materials and methods." **a** PSI complexes isolated from the WT strain of *Synechococcus* 7002 (black line), from the WT strain of *Synechococcus* 7335 grown under WL (blue line) and FRL (red line), and from the *chlF* deletion mutant of *Synechococcus* 7335 grown under WL (brown line) and FRL (purple line). **b** PSI complexes isolated from WT *Synechococcus* 7002 (black line) and from *Synechococcus* 7002 heterologously producing Chl *f* synthase from *F. thermalis* 7521. When ChlF^{7521} is produced in a WT background, the PSI complexes contain ~1 Chl *f* molecule per PSI monomer (pink line), and when ChlF^{7521} is produced in a PSII-less strain the PSI complexes contain about 3.8 Chl *f* molecules (green line)

Figure 7b depicts similar results at wavelengths from 650 to 800 nm for PSI complexes isolated from wild-type *Synechococcus* 7002 grown and from strains of *Synechococcus* 7002 that contain ~1 or 3.8 Chl *f* molecules. The data for PSI containing zero or one Chl *f* per reaction center overlaid each other, and furthermore closely resembled the response of PSI complexes from *Synechococcus* 7335 that contain only Chl *a* (compare, Fig. 7a; see Table S1). In contrast, the light response for PSI complexes from *Synechococcus* 7002 containing 3.8 Chl *f* molecules was shifted to longer wavelengths (Fig. 7b), although not by as much as for FRL–PSI from WT *Synechococcus* 7335 (compare to Fig. 7a). In particular, the amount of light required to achieve 50% photobleaching at 730 nm was only 20 times that required at the peak absorbance wavelength of 680 nm,

and 50% charge separation could be achieved at wavelengths as long as 750 nm, a wavelength about 20 nm longer than the 730 nm observed for the other two samples.

Action spectrum for photobleaching

Figure 8 represents the action spectrum for photobleaching of PSI, i.e., the effectiveness of light in producing charge separation as a function of wavelength. If the pigments that absorb the light are equally effective in producing the response, the action spectrum should overlay the absorption spectrum. Figure 8a shows that the action spectrum for light-induced photobleaching of FRL–PSI complexes of *Synechococcus* 7335 nicely overlaps the absorption spectrum of these complexes, and this is especially so in the wavelength range from 700 to 800 nm. Figure 8b shows that the action spectrum of PSI that contains 3.8 Chl *f* molecules per monomer from *Synechococcus* 7002 also largely overlaps the absorption spectrum. The ratio between the action spectrum and the visible spectrum represents the relative quantum yield and is depicted as the black line and points above the plots in both Fig. 8a, b. Comparisons of action spectra and absorption spectra of the other samples studied here are provided in Figs. S3 and S4.

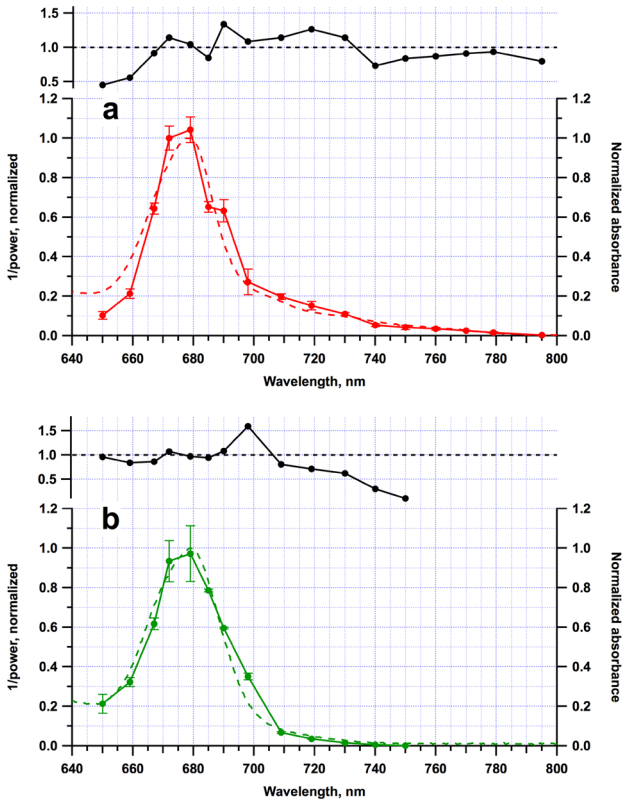

Fig. 8 Comparison of the action spectra and absorption spectra of PSI complexes. **a** Comparison of the action spectrum for light-induced photobleaching of PSI complexes isolated from the WT strain of *Synechococcus* 7335 grown under FRL (red line) compared to their absorption spectrum (dashed red line). **b** Comparison of the action spectrum for light-induced photobleaching of PSI complexes from *Synechococcus* 7002 containing 3.8 Chl *f* molecules (green line) and with their absorption spectrum (dashed green line). The absorption spectra were normalized to an absorbance of 1.0 at 678 nm, whereas the action spectra were scaled so that the error shown in the difference (black points and lines) was minimized. The error bars are largest in the regions where the pigments have the most absorption. The ratio of the action spectrum to the absorbance spectrum is plotted above each figure. This is equivalent to the relative quantum yield for the pigments absorbing in this wavelength range

Discussion

The ability of terrestrial cyanobacteria to acclimate to and utilize FRL in order to perform oxygenic photosynthesis is a highly complex process that requires the synthesis of two new Chls, Chl *d* and Chl *f*, and the coordinated expression of 20 genes, which collectively lead to extensive remodeling of PSI, PSII, and the core components of the PBS (Gan et al. 2014; Gan and Bryant 2015; Ho et al. 2017a, b, c). The evolutionary processes that were required to develop this complex response to light must be functionally and mechanistically dissected if one is to understand how nature adapted the photosynthetic apparatus to evolve this acclimation process. Furthermore, if one aspires to introduce this capability into crop plants to improve crop yields (Chen and Blankenship 2011; Blankenship and Chen 2013; Bryant 2016), it is crucial to understand which of these processes are essential and what parameters influence the efficiency of each of these modifications. In previous studies by several labs, the important roles of the modified phycobiliproteins produced in FRL have already been documented (Gan et al. 2014; Gan and Bryant 2015; Li et al. 2016; Miao et al. 2016; Xu et al. 2016, 2017; Ho et al. 2017a, b, c; Herrera-Salgado et al. 2018). These FRL-absorbing proteins, related to allophycocyanins, produce modified phycobilisomes or bicylindrical core structures (Gan et al. 2014; Li et al. 2016; Miao et al. 2016; Xu et al. 2016, 2017; Ho et al. 2017a, b, c) and strongly participate in FRL absorption by cyanobacterial cells. However, in the short term at least, because of the complexity of their biogenesis and assembly, these components of FaRLiP are unlikely to be introduced into plants.

In this study, we focused on the properties of PSI complexes produced by *Synechococcus* 7335 cells grown in WL or FRL and by *Synechococcus* 7002 cells heterologously expressing the *chlF* gene of *F. thermalis* 7521. Consistent with very recently published results of others for other FaRLiP cyanobacteria (Li et al. 2018; Nurnberg et al. 2018), we found that FRL–PSI complexes of *Synechococcus* 7335 do not contain Chl *d* and that P_{700} is most likely formed from a Chl *a*/Chl *a′* heterodimer, as found in all other studied cyanobacteria except *A. marina* (Sivakumar et al. 2003;

Tomo et al. 2008; Allakhverdiev et al. 2016). The issue of thermally activated, uphill energy transfer from Chl *d* and Chl *f* to the trapping center has been addressed in a number of studies (Mielke et al. 2013; Schmitt et al. 2018). While it is obvious that energy transfer and trapping must occur in FaRLiP cyanobacteria, if only because they are capable of growth at wavelengths at which other cyanobacteria are incapable of growing (Gan et al. 2014; Li et al. 2014; Behrendt et al. 2015), the efficiency of these processes has not been previously addressed.

Visible–near-IR absorption spectra

The absorption spectrum of PSI isolated from WT *Synechococcus* 7335 grown in far-red light shows an enhanced absorbance at wavelengths from 695 nm to 790 nm due to the presence of ~8 molecules of Chl *f*. This enhancement is absent in PSI isolated from *Synechococcus* 7335 grown in white light or in a strain of *Synechococcus* 7335 lacking Chl *f* synthase grown either in FRL or in WL, which do not synthesize Chl *f* (Table S1). When *chlF*^{7521} was introduced into *Synechococcus* 7002, the absorption spectrum of PSI showed an enhanced absorbance at wavelengths from 700 to 740 nm due to the presence of 3.8 molecules of Chl *f*, but the degree of enhancement was lower. The amino acid environment immediately surrounding the Chl-binding site(s) must play a significant role shifting the absorbance to the red. In this instance, Chl *f* bound to the PsaA/PsaB subunits in *Synechococcus* 7002 is not as red-shifted as Chl *f* bound to the PsaA2/PsaB2 subunits in *Synechococcus* 7335 expressed under far-red light conditions (Gan et al. 2014).

Light-induced difference spectrum of the trapping center

We measured the light-induced difference spectrum of the trapping center at high spectral resolution and determined that it consists of Chl *a* and not Chl *f* in WT *Synechococcus* 7335 grown under far-red light conditions and therefore probably consists of Chl *a*/Chl *a′* as in PSI complexes produced in WL that only contain Chl *a*. However, the peak of the bleaching was red-shifted 4 nm to the red, occurring at 703–704 nm rather than 699–700 nm as in WT *Synechococcus* 7335 grown under WL conditions or in *Synechococcus* 7335 that lacks ChlF grown under either WL or FRL conditions. This shift is likely due to the different amino acid environments surrounding the special pair in Chl *a* bound to the PsaA1/PsaB1 and PsaA2/PsaB2 subunits in *Synechococcus* 7335, respectively. It should be noted that a similar shift from 699 nm in WL–PSI to 702 nm in FRL–PSI in the chemical oxidized-minus-reduced difference spectrum was reported Chl *f*-containing *Halomicronema hongdechloris* (Li et al. 2018). In the absence of Chl *f* synthesis, the *chlF* null mutant of *Synechococcus* 7335 is unable to stably accumulate PSI complexes containing PsaA2 and PsaB2 (Table S2), and this explains why there is no shift into the red wavelength region even though the strain was grown in FRL. When the Chl *f* synthase gene was introduced into *Synechococcus* 7002, the maximal photobleaching still occurred at 699 to 700 nm, identical to the wild-type strain. This indicates that Chl *f* is not bound at the P_{700} binding site.

Light saturation characteristics of the trapping center

We plotted the amount of light energy required to oxidize 50% of P_{700} in PSI complexes of WT *Synechococcus* 7335 grown in FRL and WL and in PSI complexes from strains of *Synechococcus* 7002 engineered to contain Chl *f*. The data are depicted on a logarithmic scale to emphasize the differences at higher power levels. Our results showed that FRL–PSI complexes from WT *Synechococcus* 7335 are able to absorb light with wavelengths up to 40 to 50 nm longer than WL–PSI complexes and to efficiently transfer this energy to the trapping center. This is both due to the synthesis of Chl *f* and the specialized protein environments afforded by the PsaA2 and PsaB2 subunits. In the *chlF* mutant, Chl *f* as well as PsaA2 and PsaB2 are missing, and the light-induced photobleaching characteristics of PSI closely resemble those of WT *Synechococcus* 7335 grown under WL. Notably, the PSI complexes of *Synechococcus* 7002 are able to bind Chl *f* molecules heterologously produced by Chl *f* synthase. These Chl *f* molecules enhance the absorption of FRL and are capable of transferring excitation energy to the trapping center. However, the red-shift of the absorption is not nearly as large as for FRL–PSI from *Synechococcus* 7335 consistent with shifts of the light saturation curve for photobleaching ~20 nm to the red.

Finally, we plotted the action spectra PSI complexes containing Chl *f* from *Synechococcus* 7335 and *Synechococcus* 7002 and showed that it superimposes nicely with the corresponding absorbance spectra. The ratio of these two values provides the relative quantum yield for P_{700} photobleaching, and these data are plotted as the black lines and points in Fig. 8. Within the accuracy afforded by these measurements, the data confirm that for *Synechococcus* 7335, the light absorbed by Chl *f* in the wavelength range 700 to 800 nm produces a charge-separated state in PSI with a quantum yield equivalent to that of Chl *a* in the antenna. Because a determination of the absolute quantum yield of photochemistry in Chl *a*-containing PSI trimers from *Synechocystis* sp. PCC 6803 yields a value ~1.0 (Hou et al. 2001), it follows that the quantum yield of photochemistry produced by light absorbed by Chl *f* must also be close to unity. Therefore, each far-red/near-infrared photon absorbed by Chl *f* is transferred to P_{700} and results in a charge-separated state. It should be

mentioned that in addition to light harvesting, a function in the charge-separating pigments of PSI has also been proposed for Chl *f* (Kaucikas et al. 2017; Nurnberg et al. 2018). Finally, Chl *f* molecules bound PSI complexes of *Synechococcus* 7002 are also functional, but they do not extend the absorbance as far to longer wavelength, and the quantum yield appears to decrease as the wavelength increases over the range from 700 to 750 nm. These observations are in a sense expected, as it seems unreasonable that cells would have evolved the complex acclimation processes described above if a single gene product could replace the function of many genes affecting several different components of the photosynthetic apparatus. As noted above, these results are directly relevant to the issue of extending the wavelength range for photosynthesis in crop plants as a mechanism for enhancing photosynthetic efficiency (Chen and Blankenship 2011; Blankenship and Chen 2013; Bryant 2016). The results obtained here suggest that, while this might be possible simply by heterologously expressing the *chlF* gene in plants, to achieve optimal FRL utilization may require specific engineering of Chl-binding proteins to increase the efficiency of excitation energy transfer and trapping.

Acknowledgements This work was supported by the National Science Foundation Grant MCB-1613022 to D.A.B and J.H.G. This research was also conducted under the auspices of the Photosynthetic Antenna Research Center (PARC), an Energy Frontier Research Center funded by the DOE, Office of Science, Office of Basic Energy Sciences under Award Number DE-SC 0001035 (D.A.B.).

Compliance with ethical standards

Conflict of interest The authors declare that they have no conflict of interest.

References

Airs RL, Temperton B, Sambles C, Farnham G, Skill SC, Llewellyn CA (2014) Chlorophyll *f* and chlorophyll *d* are produced in the cyanobacterium *Chlorogloeopsis fritschii* when cultured under natural light and near-infrared radiation. FEBS Lett 588:3770–3777

Allakhverdiev SI, Tomo T, Shimada Y, Kindo H, Nagao R, Klimov VV, Mimuro M (2010) Redox potential of pheophytin *a* in photosystem II of two cyanobacteria having the different special pair chlorophylls. Proc Natl Acad Sci USA 107:3924–3929

Allakhverdiev SI, Kreslavski VD, Zharmukhamedov SK, Voloshin RA, Korol'kova DV, Tomo T, Shen JR (2016) Chlorophylls *d* and *f* and their role in primary photosynthetic processes of cyanobacteria. Biochemistry (Moscow) 81:201–212

Behrendt L, Brejnrod A, Schliep M, Sørensen SJ, Larkum AWD, Kühl M (2015) Chlorophyll *f*-driven photosynthesis in a cavernous cyanobacterium. ISME J 9:2108–2111

Blankenship RE, Chen M (2013) Spectral expansion and antenna reduction can enhance photosynthesis for energy production. Curr Opin Chem Biol 17:457–461

Bryant DA (2016) Improving crop yields and algal biofuel production by expanding the wavelength range for photosynthesis. Information Systems for Biotechnology News Report pp 1–6

Chen M (2014) Chlorophyll modifications and their spectral extension in oxygenic photosynthesis. Ann Rev Biochem 83:217–340

Chen M, Blankenship RE (2011) Expanding the solar spectrum used by photosynthesis. Trends Plant Sci 16:427–431

Cherepanov DA, Shelaev IV, Gostev FE, Mamedov MD, Petrova AA, Aybush AV, Shuvalov VA, Semenov AY, Nadtochenko VA (2017a) Excitation of photosystem I by 760 nm femtosecond laser pulses: transient absorption spectra and intermediates. J Phys B 50:174001

Cherepanov DA, Shelaev IV, Gostev FE, Mamedov MD, Petrova AA, Aybush AV, Shuvalov VA, Semenov AY, Nadtochenko VA (2017b) Mechanism of adiabatic primary electron transfer in photosystem I: femtosecond spectroscopy upon excitation of reaction center in the far-red edge of the Qy band. Biochim Biophys Acta 1858:895–905

Gan F, Bryant DA (2015) Adaptive and acclimative responses of cyanobacteria to far-red light. Environ Microbiol 17:3450–3465

Gan F, Zhang S, Rockwell NC, Martin SS, Lagarias JC, Bryant DA (2014) Extensive remodeling of a cyanobacterial photosynthetic apparatus in far-red light. Science 345:1312–1317

Golbeck J (2006) Photosystem I: the light-driven plastocyanin:ferredoxin oxidoreductase. Springer, Dordrecht

Golbeck J, Bryant D (1991) Photosystem-I. Curr Topics Bioenerg 16:83–177

Grotjohann I, Fromme P (2005) Structure of cyanobacterial photosystem I. Photosynth Res 85:51–72

Herrera-Salgado P, Leyva-Castillo LE, Rios-Castro E, Gomez-Lojero C (2018) Complementary chromatic and far-red photoacclimations in *Synechococcus* ATCC 29403 (PCC 7335). I: the phycobilisomes, a proteomic approach. Photosynth Res 138:39–56

Ho M-Y (2018) Characterization of far-red light photoacclimation in cyanobacteria. Biochem Mol Biol 131:173–186

Ho M-Y, Shen G, Canniffe DP, Zhao C, Bryant DA (2016) Light-dependent chlorophyll *f* synthase is a highly divergent paralog of PsbA of photosystem II. Science 353:213–227

Ho M-Y, Gan F, Shen GZ, Bryant DA (2017a) Far-red light photoacclimation (FaRLiP) in *Synechococcus* sp. PCC 7335. II. Characterization of phycobiliproteins produced during acclimation to far-red light. Photosynth Res 131:187–202

Ho M-Y, Gan F, Shen GZ, Zhao C, Bryant DA (2017b) Far-red light photoacclimation (FaRLiP) in *Synechococcus* sp. PCC 7335: I. regulation of FaRLiP gene expression. Photosynth Res 131:173–186

Ho M-Y, Soulier NT, Canniffe DP, Shen G, Bryant DA (2017c) Light regulation of pigment and photosystem biosynthesis in cyanobacteria. Curr Opin Plant Biol 37:24–33

Hou JM, Boichenko VA, Wang YC, Chitnis PR, Mauzerall D (2001) Thermodynamics of electron transfer in oxygenic photosynthetic reaction centers: a pulsed photoacoustic study of electron transfer in photosystem I reveals a similarity to bacterial reaction centers in both volume change and entropy. Biochemistry 40:7109–7116

Itoh S, Mino H, Itoh K, Shigenaga T, Uzumaki T, Iwaki M (2007) Function of chlorophyll *d* in reaction centers of photosystems I and II of the oxygenic photosynthesis of *Acaryochloris marina*. Biochemistry 46:12473–12481

Jordan P, Fromme P, Witt HT, Klukas O, Saenger W, Krauß N (2001) Three dimensional structure of Photosystem I at 2.5 Å resolution. Nature 411:909–917

Kaucikas M, Nurnberg D, Dorlhiac G, Rutherford AW, van Thor JJ (2017) Femtosecond visible transient absorption spectroscopy of chlorophyll *f*-containing photosystem I. Biophys J 112:234–249

Kok B (1956) On the reversible absorption change at 705 nm in photosynthetic organisms. Biochim Biophys Acta 22:399–401

Kumazaki S, Abiko K, Ikegami I, Iwaki M, Itoh S (2002) Energy equilibration and primary charge separation in chlorophyll *d*-based photosystem I reaction center isolated from *Acaryochloris marina*. FEBS Lett 530:153–157

Lambert DH, Stevens SE Jr (1986) Photoheterotrophic growth of *Agmenellum quadruplicatum* PR-6. J Bacteriol 165:654–656

Li Y, Scales N, Blankenship RE, Willows RD, Chen M (2012) Extinction coefficient for red-shifted chlorophylls: chlorophyll *d* and chlorophyll *f*. Biochim Biophys Acta 1817:1292–1298

Li Y, Lin Y, Loughlin PC, Chen M (2014) Optimization and effects of different culture conditions on growth of *Halomicronema hongdechloris* - a filamentous cyanobacterium containing chlorophyll *f*. Front Plant Sci 5:67

Li Y, Lin Y, Garvey CJ, Birch D, Corkery RW, Loughlin PC, Scheer H, Willows RD, Chen M (2016) Characterization of red-shifted phycobilisomes isolated from the chlorophyll *f*-containing cyanobacterium *Halomicronema hongdechloris*. Biochim Biophys Acta 1857:107–114

Li Y, Vella N, Chen M (2018) Characterization of isolated photosystem I from *Halomicronema hongdechoris*, a chlorophyll *f*-producing cyanobacterium. Photosynthetica 56:306–315

Lichtenthaler HK (1987) Chlorophylls and carotenoids: Pigments of photosynthetic biomembranes. Methods Enzymol 148:350–382

Ludwig M, Bryant DA (2011) Transcription profiling of the cyanobacterium *Synechococcus* sp. PCC 7002 using high-throughput cDNA sequencing. Front Microbiol 2:41

Miao D, Ding WL, Zhao BQ, Lu L, Xu QZ, Scheer H, Zhao KH (2016) Adapting photosynthesis to the near-infrared: non-covalent binding of phycocyanobilin provides an extreme spectral red-shift to phycobilisome core-membrane linker from *Synechococcus* sp. PCC 7335. Biochim Biophys Acta 1857:688–694

Mielke SP, Kiang NY, Blankenship RE, Mauzerall D (2013) Photosystem trap energies and spectrally-dependent energy-storage efficiencies in the Chl *d*-utilizing cyanobacterium, *Acaryochloris marina*. Biochim Biophys Acta 1827:255–265

Miyashita H, Ikemoto H, Kurano N, Adachi K, Chihara M, Miyachi S (1996) Chlorophyll *d* as a major pigment. Nature 383:402

Muller MG, Slavov C, Luthra R, Redding KE, Holzwarth AR (2010) Independent initiation of primary electron transfer in the two branches of the Photosystem I reaction center. Proc Natl Acad Sci USA 107:4123–4128

Nurnberg DJ, Morton J, Santabarbara S, Telfer A, Joliot P, Antonaru LA, Ruban AV, Cardona T, Krausz E, Boussac A, Fantuzzi A, Rutherford AW (2018) Photochemistry beyond the red limit in chlorophyll *f*-containing photosystems. Science 360:1210–1213

Ortega-Ramos M, Canniffe DP, Radle M, Neil Hunter C, Bryant DA, Golbeck JH (2018) Engineered biosynthesis of bacteriochlorophyll g_F in R*hodobacter sphaeroides*. Biochim Biophys Acta 1859:501–509

Razeghifard MR, Chen M, Hughes JL, Freeman J, Krausz E, Wydrzynski T (2005) Spectroscopic studies of photosystem II in chlorophyll *d*-containing *Acaryochloris marina*. Biochemistry 44:11178–11187

Rippka R, Deuuelles J, Waterbury JB, Herdman M, Stanier RY (1979) Generic assignments, strain histories and properties of pure cultures of cyanobacteria. J Gen Microbiol 111:1–61

Schlodder E, Cetin M, Eckert HJ, Schmitt FJ, Barber J, Telfer A (2007) Both chlorophylls *a* and *d* are essential for the photochemistry in photosystem II of the cyanobacteria, *Acaryochloris marina*. Biochim Biophys Acta 1767:589–595

Schluchter WM, Shen GH, Zhao JD, Bryant DA (1996) Characterization of *psaI* and *psaL* mutants of *Synechococcus* sp strain PCC 7002: a new model for state transitions in cyanobacteria. Photochem Photobiol 64:53–66

Schmitt FJ, Campbell ZY, Bui MV, Huls A, Tomo T, Chen M, Maksimov EG, Allakhverdiev SI, Friedrich T (2018) Photosynthesis supported by a chlorophyll *f*-dependent, entropy-driven uphill energy transfer in *Halomicronema hongdechloris* cells adapted to far-red light. Photosynth Res. https://doi.org/10.1007/s11120-11018-10556-11122

Shen GZ, Bryant DA (1995) Characterization of a *Synechococcus* sp strain PCC 7002 mutant lacking Photosystem I. Protein assembly and energy distribution in the absence of the Photosystem I reaction center core complex. Photosynth Res 44:41–53

Shen G, Zhao J, Reimer SK, Antonkine ML, Cai Q, Weiland SM, Golbeck JH, Bryant DA (2002) Assembly of Photosystem I. I. Inactivation of the *rubA* gene encoding a membrane-associated rubredoxin in the cyanobacterium *Synechococcus* sp. PCC 7002 causes a loss of Photosystem I activity. J Biol Chem 277:20343–20354

Shen G, Schluchter WM, Bryant DA (2008) Biogenesis of phycobiliproteins: I. *cpcS*-I and *cpcU* mutants of the cyanobacterium *Synechococcus* sp. PCC 7002 define a heterodimeric phyococyanobilin lyase specific for beta-phycocyanin and allophycocyanin subunits. J Biol Chem 283:7503–7512

Shen G, Gan F, Bryant DA (2016) The siderophilic cyanobacterium *Leptolyngbya* sp. strain JSC-1 acclimates to iron starvation by expressing multiple *isiA*-family genes. Photosynth Res 128:325–340

Shen G, Canniffe DP, Ho M-Y, Kurashov V, Golbeck JH, Bryant DA (2019) Characterization of chlorophyll *f* synthase heterologously produced in *Synechococcus* sp. PCC 7002. Photosynth Res. https://doi.org/10.1007/s11120-018-00610-9

Sivakumar V, Wang R, Hastings G (2003) Photo-oxidation of P740, the primary electron donor in photosystem I from *Acaryochloris marina*. Biophys J 85:3162–3172

Tomo T, Okubo T, Akimoto S, Yokono M, Miyashita H, Tsuchiya T, Noguchi T, Mimuro M (2007) Identification of the special pair of photosystem II in a chlorophyll *d*-dominated cyanobacterium. Proc Natl Acad Sci USA 104:7283–7288

Tomo T, Kato Y, Suzuki T, Akimoto S, Okubo T, Noguchi T, Hasegawa K, Tsuchiya T, Tanaka K, Fukuya M, Dohmae N, Watanabe T, Mimuro M (2008) Characterization of highly purified photosystem I complexes from the chlorophyll *d*-dominated cyanobacterium *Acaryochloris marina* MBIC 11017. J Biol Chem 283:18198–18209

Webber AN, Lubitz W (2001) P700: the primary electron donor of Photosystem I. Biochim Biophys Acta 1507:61–79

Xu QZ, Han JX, Tang QY, Ding WL, Miao D, Zhou M, Scheer H, Zhao KH (2016) Far-red light photoacclimation: Chromophorylation of FR induced alpha- and beta-subunits of allophycocyanin from *Chroococcidiopsis thermalis* sp. PCC7203. Biochim Biophys Acta 1857:1607–1616

Xu QZ, Tang QY, Han JX, Ding WL, Zhao BQ, Zhou M, Gartner W, Scheer H, Zhao KH (2017) Chromophorylation (in *Escherichia coli*) of allophycocyanin B subunits from far-red light acclimated *Chroococcidiopsis thermalis* sp. PCC7203. Photochem Photobiol Sci 16:1153–1161

Zhao C, Gan F, Shen G, Bryant DA (2015) RfpA, RfpB, and RfpC are the master control elements of far-red light photoacclimation (FaRLiP). Front Microbiol 6:1303

Publisher's Note Springer Nature remains neutral with regard to jurisdictional claims in published maps and institutional affiliations.